Rheology of Supercooled P-Se Glass-forming Liquids: From Networks to Molecules and the Emergence of Power-Law Relaxation Behavior

[1]Bing Yuan, [2]Bruce Aitken, [1]Sabyasachi Sen*

[1]*Department of Materials Science & Engineering, University of California at Davis,*

Davis, CA 95616, USA

[2]*Science & Technology Division, Corning Inc., Corning, NY 14831, USA*

*Corresponding Author: Sabyasachi Sen (email: sbsen@ucdavis.edu)

ABSTRACT

The effect of the network-to-molecular structural transformation with increasing phosphorus content in P_xSe_{100-x} ($30 \leq x \leq 67$) supercooled liquids on their shear-mechanical response is investigated using oscillatory shear rheometry. While network liquids with $30 \leq x \leq 40$ are characterized by shear relaxation via a network bond scission/renewal process, a Maxwell scaling of the storage (G′) and loss (G") shear moduli and a frequency-independent viscosity at low frequencies, a new relaxation process emerges in liquids with intermediate compositions ($45 \leq x \leq 50$). This process is attributed to an interconversion between network and molecular structural moieties. Predominantly molecular liquids with $x \geq 63$, on the other hand, are characterized by a departure from the Maxwell behavior as the storage modulus shows a linear frequency scaling $G'(\omega) \sim \omega$ over nearly the entire frequency range below the G′-G" crossover and a nearly constant ratio of G″/G′ in the terminal region. Moreover, the dynamic viscosity of these rather fragile molecular liquids shows significant enhancement over that of network liquids at frequencies below the dynamical onset and does not reach a frequency-independent regime even at frequencies that are four orders of magnitude lower than that of the onset. Such power-law relaxation behavior of the molecular liquids is ascribed to an extremely broad distribution of relaxation timescales with the coexistence of rapid rotational motion of individual molecules and cooperative dynamics of transient molecular clusters, with the latter being significantly slower than the shear relaxation timescale.

1. INTRODUCTION

The processing of glasses from their parent supercooled liquids is critically dependent on the rheological behavior of the latter. Moreover, the frequency ω dependence of the shear mechanical response, including the storage and loss shear moduli (G' and G'', respectively) and viscosity η, of glass-forming liquids sheds light on the atomistic details of the relaxation processes associated with the glass transition and related phenomena. The shear mechanical response and modes of structural relaxation of a supercooled liquid critically depends on the nature of the structural moieties and the resulting dimensionality and connectivity of the network (e.g. isolated vs. associated molecules, 1-D chains or 3-D polyhedral network).[1,2] For example, the primary or α-relaxation of polymeric chain liquids is controlled by the segmental motion of the constituent chains, while the motion of the covalently bonded backbone structure gives rise to the slowest relaxation mode in these systems.[3] In contrast, a significantly simple rheological behavior is displayed by the archetypal 3D network oxide liquids such as silicates and borates, where the structural relaxation is controlled by the bond scission/renewal based reconfiguration of the network. Correspondingly the shear mechanical response of these liquids shows a "simple liquid" behavior with a single G'-G'' crossover at high frequency and a Maxwell scaling of $G(\omega) \sim \omega^n$ at low frequencies in the terminal regime, with $n = 2$ and 1 for G' and G'', respectively.[4,5] Such simple behavior is also displayed by the non-associated organic molecular glass-forming liquids such as tris-naphthylbenzene, where the viscosity and structural relaxation of the supercooled liquid involve local flow processes of the constituent molecules that redistribute the free volume.[6,7] On the other hand, seemingly simple molecular liquids such as monohydroxy alcohols and various other low-molecular-weight hydrogen bonded liquids have shown intense Debye relaxation modes in their rheological spectra that are slower than the structural relaxation, which lead to significant viscosity enhancement.[7,8] Nuclear magnetic resonance (NMR) spectroscopic studies indicated that these modes in monohydroxy alcohols were related to the restructuring of transient chains formed via hydrogen bonding between molecules.[9]

The compositional evolution of the shear mechanical response of glass-forming chalcogenide liquids is particularly interesting since the structure of these liquids can be tuned, as a function of composition, from being predominantly molecular, all the way to a 3D network. Previous systematic small-amplitude oscillatory shear (SAOS) rheometry studies on binary selenide liquids in the As-Se, Ge-Se and P-Se systems[10–13] have shown that the structural relaxation of Se-rich liquids consisting of $[\text{-Se-}]_n$ chain-like structural moieties is characterized by the coexistence of a slow Debye-like process and a fast process. ^{77}Se dynamical nuclear magnetic resonance (NMR) spectroscopic studies[14] have indicated that the slow process corresponds to the bond scission/renewal induced $[\text{-Se-}]_n$ chain restructuring in the structure, while the fast process is associated with the segmental dynamics of these chains. The addition of Ge, As or P to Se leads to cross-linking of these chains and their effective shortening. Consequently, the segmental dynamics disappear at a Ge/As/P concentration where the chain length becomes too short to sustain the segmental dynamics and the structural network becomes sufficiently cross-linked and rigid. At this stage the structural relaxation is controlled by the bond scission/renewal induced restructuring of the emerging network and correspondingly the shear mechanical response shows a behavior similar to that characteristic of the archetypal network oxide liquids mentioned above.

A significant departure from this evolutionary scheme of rheological behavior has recently been reported in Ge-As sulfide glass-forming liquids where a progressive increase of the molecule : network ratio in the structure resulted in a monotonic lowering of n from 2 for to 1 for the scaling of $G'(\omega) \sim \omega^n$ in the entire low frequency regime below the G′-G" crossover.[15] Moreover, at the highest molecule content the ratio G"/G′ reached a nearly constant value and the liquid did not display a purely viscous response even at the lowest frequencies. It may be noted that, while such power-law rheological behavior has not been observed in non-associated organic molecular glass-forming liquids such as tris-naphthylbenzene, it has been extensively reported in widely different classes of soft matter including gels, elastomers, biomaterials and composites.[16] Although the phenomenological soft glassy rheology model captures the range of this behavior well, an atomistic explanation remains missing in the literature to date.[17] Moreover, the generality of this power-law relaxation behavior in other non-associated molecular inorganic glass forming liquids remains to be explored. Here we report the results of a rheological study of P_xSe_{100-x} supercooled liquids with $30 \leq x \leq 67$ to investigate the effects of the network-to-molecular transformation on their shear-mechanical response and to explore the generality of the power-law shear mechanical response in non-associated molecular chalcogenides. The corresponding compositional evolution of the structural relaxation mechanisms and their effect on viscous flow are discussed.

2. EXPERIMENTAL

2.1 Sample Synthesis

The P_xSe_{100-x} glasses ($30 \leq x \leq 67$) were synthesized in ~12g batches using the conventional melt-quench method. For $30 \leq x \leq 50$, constituent elements, red phosphorus (Spectrum, 99.999%) and selenium (Alfa Aesar, 99.999%), were loaded in evacuated (10^{-4} Torr) quartz ampoules and then placed in a rocking furnace, slowly heated to 873K over 13 hours and held at this temperature for 36 h to ensure melt homogeneity. The melts were finally quenched to form glass by dipping the ampoules in water. The predominantly molecular glasses $P_{63}Se_{37}$ and $P_{67}Se_{33}$ were prepared in similar fashion but the ampoules were cooled to 623K and held at this temperature for 30 minutes prior to quenching.

2.2. Parallel Plate Rheometry

The rheological measurements of all compositions were carried out on an Anton-Paar MCR 92 parallel plate rheometer equipped with a Peltier heater (up to 200 ºC) under constant nitrogen gas flow. The samples were prepared by first rapidly heating them inside the rheometer to the softening point and then pressing between the upper oscillatory plate (8mm diameter) and the lower stationary plate and trimming to a disk-like shape with a thickness of ~ 1 mm. For SAOS measurements the samples were allowed to equilibrate at each desired measurement temperature followed by the determination of the linear viscoelastic region. During the SAOS measurement, a sinusoidal strain was applied with varying angular frequency ω between 1 to 600 rad/s and the induced torque was recorded to calculate the storage and loss moduli G´and G˝ as a function of ω. Measurements were carried out at multiple temperatures for each sample and master curves of G′(ω) and G"(ω) were constructed using time-temperature superposition (TTS). The dynamic viscosity was calculated from the relation $\eta' = \frac{G"}{\omega}$.

The Newtonian viscosity η of two compositions with x = 63 and 67 was measured using steady shear for $\eta \leq 10^9$ Pa.s and using creep for $\eta \geq 10^{10}$ Pa.s. The Newtonian viscosity was determined in the steady shear measurements as the ratio of stress to strain rate at various strain rates $\dot{\gamma}$ ranging between 0.01 s^{-1} and 1 s^{-1} at each temperature. For creep measurements, a constant shear stress τ was applied to the thermally equilibrated sample while the strain response was constantly monitored as a function of time. The viscosity is obtained from the relation $\eta = \frac{\tau}{\dot{\gamma}}$ in the steady-state region where the strain rate $\dot{\gamma}$ no longer changes with time.

3. RESULTS AND DISCUSSION

Previous structural studies of P_xSe_{100-x} glasses based on Raman and multi-nuclear (^{31}P and ^{77}Se) NMR spectroscopy[18–25] have conclusively shown that the structure of the Se-rich liquids in this system consists predominantly of $[\text{-Se-}]_n$ chains. Progressive addition of P results in cross-linking and shortening of the Se chain segments to form a 3D network. Such a compositional evolution of structure continues up to $x \sim 50$ and is broadly similar to those observed in As-Se and Ge-Se systems. However, further increase in P content results in the formation of P_4Se_3 molecules and the structure becomes predominantly molecular for $x \geq 63$. The temperature-dependent G′ and G″ spectra of all P_xSe_{100-x} supercooled liquids in the composition range $30 \leq x \leq 67$are shown in Fig. 1a. At each temperature, only a portion of the whole spectrum is revealed within the observation window of the rheometer. These spectra gradually shift from low to high frequency with increasing temperature, which enables a sequential observation of a wide frequency range. The experimental master curves of $G'(\omega)$ and $G''(\omega)$ constructed using time-temperature superposition (TTS) for all P_xSe_{100-x} supercooled liquids, at temperatures corresponding to the isokom of approximately ~ 10^9 Pa.s, are shown in Figure 1b. At high frequencies the $G'(\omega)$ in these master curves reaches a plateau corresponding to the glassy modulus G_∞ , which is ~ 1.3 to 1.5 GPa for the network liquids with $30 \leq x \leq 40$, while it drops by 50% (0.7 – 0.8 GPa) for the molecular $P_{63}Se_{37}$ and $P_{67}Se_{33}$ liquids. This change in G_∞ is consistent with a drastic lowering of the structural connectivity in the latter liquids resulting from the formation of P_4Se_3 molecules, which are held together in the structure via weak intermolecular van der Waals bonding.[18] It is apparent that the network liquids with composition $30 \leq x \leq 40$ display a normal behavior with a single relaxation process and Maxwell scaling of G′ and G" in the terminal regime. This primary relaxation process in liquids with compositions ranging between $15 \leq x \leq 25$ was assigned in a previous study to P-Se and Se-Se bond scission/renewal.[13] Such a process is likely to remain active and responsible for structural relaxation in liquids with $30 \leq x \leq 40$. However, the viscoelastic spectra for the $P_{45}Se_{55}$ and $P_{50}Se_{50}$ liquids show a clear and relatively abrupt change in the frequency dependence of G′ from $n = 2$ in the terminal regime to $n \sim 1$ for G′ values above a few MPa (Fig. 1b). Therefore, these liquids are characterized by two relaxation processes and the change in slope with increasing frequency to $n \sim 1$ suggests the emergence of a new relaxation mode. Previous studies have demonstrated that the network structure of P_xSe_{100-x} glasses with $45 \leq x \leq 50$ consists primarily of ethylene-like $_{2/2}SeP–PSe_{2/2}$ units that are expected to form 2D corrugated sheet-like superstructural moieties.[18,19] Moreover, ^{31}P and ^{77}Se dynamical NMR studies[26–28] in the literature have shown that the bond scission/renewal dynamics in these liquids are associated with interconversion between different P sites that can be represented in the form of the reaction: $3P_2(Se_{1/2})_4 \leftrightarrow 2P(Se_{1/2})_3 + P_4Se_3$. Such an interconversion between the network and molecular (P_4Se_3) topological elements would result in a change in the intermediate-range structure and is expected to appear as a separate relaxation mode in the viscoelastic spectrum, consistent with the experimental observation.

In contrast to these predominantly network P_xSe_{100-x} liquids, the viscoelastic spectra of the P_4Se_3 molecule-rich $P_{63}Se_{37}$ and $P_{67}Se_{33}$ liquids display a rather different behavior where the ω dependences of G′ and G″ are parallel and both follow a slope of $n =1$ in the terminal region. As noted earlier, this frequency dependence of G′ and G″ and the nearly constant ratio of G″/G′ in the terminal region are the signatures of a power-law relaxation behavior of a wide variety of soft matter, including and most notably gels near their critical point, which are characterized by a broad distribution of structural length scales and relaxation timescales.[29] The validity of this hypothesis is tested here by comparing the relaxation time spectra H(τ) of the normally behaving $P_{30}Se_{70}$

network liquid with that of the molecular $P_{63}Se_{37}$ liquid (Fig. 2). The H(τ) spectrum can be derived in principle from the corresponding G′(ω) or G″(ω) data using one of the following relations with G_0 being the equilibrium modulus.:

$$G'(\omega) = G_0 + \int_{-\infty}^{\infty} \frac{\omega^2\tau^2}{1+\omega^2\tau^2} H \, d \, ln \, \tau$$

$$G''(\omega) = \int_{-\infty}^{\infty} \frac{\omega\tau}{1+\omega^2\tau^2} H \, d \, ln \, \tau$$

Therefore, the determination of H(τ) requires inversion of these relations and calculation of derivatives of G′(ω) or G″(ω) with respect to ln ω. Instead, here the H(τ) spectra are calculated without taking these derivatives, following Ninomiya and Ferry's approximate method that employs a numerical differencing procedure[30]. This method requires values of G′(ω) spaced at equal intervals on a log frequency scale above and below the frequency ω = 1/τ at which H(τ) is calculated, e.g. G′(ω) values can be taken at frequencies ω/a^2, ω/a, ω, $a\omega$, and $a^2\omega$, where a is a constant multiplier. Then H(τ) can be approximated as:

$$H(\tau) = \frac{G'(a\omega) - G'(\omega/a)}{2\ln a} - \frac{a^2}{(a^2-1)^2} \frac{G'(a^2\omega) - G'(\omega/a^2) - 2G'(a\omega) + 2G'(\omega/a)}{2\ln a}\Bigg|_{1/\omega=\tau} \tag{1}$$

A value of log a = 0.25 is used in the present calculations as a careful evaluation of this numerical method has shown that log a needs to be in the range 0.2-0.4 for an accurate approximation of H(τ), as larger values lead to poor approximation and smaller values lead to large fluctuations in the differencing result.[30] It is clear from Fig. 2 that the H(τ) spectrum of the $P_{63}Se_{37}$ liquid is significantly broader than that of the $P_{30}Se_{70}$ liquid, with the former displaying an extended long-time tail and a plateau on the short-time side (Fig. 2). This behavior of the $P_{63}Se_{37}$ liquid is remarkably similar to that observed in a previous study for the molecular $Ge_3As_{52}S_{45}$ liquid, which contains As_4S_3 cage molecules (Fig. 2).[15] The broadening of H(τ) at short times or high frequencies is consistent with the results of a previous two-dimensional ^{31}P NMR study[31] that has shown that the constituent P_4Se_3 molecules in the $P_{63}Se_{37}$ liquid perform rapid isotropic rotational reorientation at timescales that are orders of magnitude faster than the shear relaxation time scale in the supercooled region. This strongly temporally decoupled rotation of individual molecules continues in the glassy state and is reminiscent of the situation in plastic crystals where the constituent molecules perform rapid rotation at the lattice sites.[31–33] On the other hand, the long-time tail of H(τ) characteristic of this liquid may be attributed to correlated reorientation dynamics in transient molecular clusters.

Further insights into the relaxation time distribution can be obtained by simulating the viscoelastic spectra of the $P_{30}Se_{70}$ network and $P_{63}Se_{37}$ molecular liquids using the Havriliak-Negami (H-N) function for the frequency dependence of the complex modulus $G^*(\omega)$:[34]

$$G^*(\omega) = G_\infty + (G_0 - G_\infty)\frac{1}{[1+(i\omega\tau_H)^\alpha]^\beta};\ \ 0 < \alpha,\ \alpha\beta < 1 \qquad (2)$$

where G_∞ and G_0 are the infinite frequency glassy shear modulus and the zero-frequency modulus, and τ_H, α and β represent the characteristic H-N relaxation time, broadness, and asymmetry of the corresponding relaxation time distribution, respectively. The H-N equation reduces to the Cole-Davidson distribution for $\alpha = 1$ and the Cole-Cole distribution for $\beta = 1$. It may be noted that although the H-N function takes the limiting values of the dynamic shear modulus to zero at low frequencies and to a plateau at G_∞ for high frequencies as required for an α-relaxation process, the viscosity does not reach a frequency-independent regime at a finite low-frequency limit. The latter outcome is indeed characteristic of gels.[16,29] The simulations of the viscoelastic spectra of the $P_{30}Se_{70}$ and $P_{63}Se_{37}$ liquids with the H-N function are shown in Fig. 3. Both the Maxwell scaling in the terminal regime, characteristic of the network liquid, and the "anomalous" scaling of $G' \sim \omega$ exhibited by the molecular liquids are captured well using the H-N function. While the viscoelastic spectrum of the network $P_{30}Se_{70}$ liquid can be fitted with α =1.0 and β = 0.32, i.e. the Cole-Davidson model, that of the molecular $P_{63}Se_{37}$ liquid can only be simulated with considerably smaller α (= 0.82) and β (= 0.13) values, suggesting that the relaxation time spectrum of the latter is significantly broader and more asymmetric compared to that of the former liquid. The corresponding probability density function of the log-relaxation time $h_{HN}(\log \tau)$ for these two liquids can be obtained using the following relations:

$$h_{HN}(\log \tau) = \frac{1}{A\pi} \frac{\sin(\beta\Psi)}{((\tau\omega_H)^{-2\alpha}+2(\tau\omega_H)^{-\alpha}\cos(\pi\alpha)+1)^{\frac{\beta}{2}}}$$

$$\Psi = \frac{\pi}{2} - \arctan\left(\frac{(\tau\omega_H)^{\alpha}+\cos(\pi\alpha)}{\sin(\pi\alpha)}\right) \tag{3}$$

where $A = (\ln 10)^{-1}$ and $\omega_H = 1/\tau_H$ is the characteristic H-N relaxation frequency. The calculated $h_{HN}(\log \tau)$ spectra show that the relaxation time distribution of the $P_{30}Se_{70}$ liquid indeed exhibits a less skewed and narrower peak whereas that of the $P_{63}Se_{37}$ molecular liquid show displays a rather broad and highly skewed distribution with an extended short-time tail (Fig. 4). The broad distribution of relaxation times for the molecular liquids is indicative of the presence of a correspondingly complex potential energy landscape (PEL) with a wide range of barrier heights separating the metabasins. Such a PEL is characteristic of liquids with high fragility index *m*, where $m = \left.\frac{d\log_{10}\eta}{d(T_g/T)}\right|_{T=T_g}$, and T_g is the glass transition temperature.[35]

The fragility index of the two molecular liquids $P_{63}Se_{37}$ and $P_{67}Se_{33}$ is obtained by fitting the temperature dependence of their viscosity as determined in this study (Fig. 5) with the MYEGA equation:[36,37]

$$log\,\eta = log_{10}\eta_\infty + \frac{K}{T}\cdot exp\,(\frac{C}{T}) \tag{4}$$

where $log_{10}\eta_\infty$, K, and C are all fitting parameters. The corresponding fragility index *m* is calculated from these fitting parameters using the following relation

$$m = \left(\frac{K}{T_g}\right)\left(1+\frac{C}{T_g}\right)\exp\left(\frac{C}{T_g}\right) \tag{5}$$

where the T_g of the binary P-Se glasses were obtained from previous reports in the literature.[18,38] It may be noted that the T_g of the molecular P-Se glasses are much lower than their network counterparts, consistent with the formation of P_4Se_3 molecules that drastically lowers the connectivity of the structure.[18] These calculations yield quite high values of *m* ranging between 65 and 75 for these molecular liquids, indicating that these liquids are significantly more fragile than their network counterparts with $25 \leq x \leq 50$, that are characterized by $m \sim 35 \pm 5$.[13]

The unusual shear-mechanical response of the molecular P-Se liquids is further explored in their dynamic viscosity $\eta'(\omega)$ behavior in a scaled viscosity $Z(\omega)$ vs. normalized frequency ω/ω_{max} plot (Fig. 6). Here ω_{max} is the frequency corresponding to the maximum in G″ and $Z(\omega)$ is defined as:

$$Z(\omega) = \frac{\eta'(\omega)}{(G_\infty/\omega_{max})} \tag{6}$$

It may be noted that (G_∞/ω_{max}) is equal to $\eta'(\omega \sim \omega_{max})$, which corresponds to the stress relaxation process. It is evident from Fig. 6 that $Z(\omega)$ for the network P_xSe_{100-x} liquids with $30 \leq x \leq 50$ reaches the frequency independent region below $\omega/\omega_{max} \sim 0.1$. Such behavior is characteristic of a wide range of network and unassociated molecular glass-forming liquids.[7,15] In contrast, the molecular P_xSe_{100-x} liquids with $x = 63$ and 67 show clear viscosity enhancement over the normal network liquids in the low-frequency region below $\omega/\omega_{max} \sim 1$ with a frequency scaling of $Z(\omega) \sim (\omega/\omega_{max})^{-0.12}$ (Fig 6). Moreover, like gels, the dynamic viscosity of these molecular liquids does not reach a frequency independent regime even at the lowest frequencies of measurement ($\omega/\omega_{max} \sim 10^{-4}$) accessed in the present study, consistent with the presence of ultraslow relaxation processes in these liquids with timescales significantly longer than that of shear relaxation.

Indications for the existence of ultraslow relaxation processes are also apparent when one compares the van Gurp – Palmen (vGP) plot of the phase angle δ vs. $|G^*|$ of the $P_{30}Se_{70}$ network liquid with that of the $P_{63}Se_{37}$ molecular liquid (Fig. 7). Here, by definition, $\tan\delta = G''/G'$ and $|G^*| = \sqrt{G'^2 + G''^2}$. It is clear from Fig. 7 that, while δ of the $P_{30}Se_{70}$ liquid reaches a value of ~90° at low frequencies characteristic of a purely viscous response in the terminal regime, that of the $P_{63}Se_{37}$ liquid plateaus out at ~80°, implying that a purely viscous response is not obtained even at the lowest frequencies of measurement. As noted earlier and shown in Fig. 7, a similar viscoelastic behavior was recently reported in another molecular liquid of composition $Ge_3As_{52}S_{45}$.[15] Therefore, similar to gels at their critical point, a small elastic component of the shear-mechanical response remains present at these frequencies in these molecular liquids, which therefore persist in a state intermediate between a liquid and a solid.

4. CONCLUSIONS

The compositional evolution of the viscoelastic response of of P_xSe_{100-x} ($30 \leq x \leq 67$) supercooled liquids is found to be correlated with the accompanying network-to-molecular structural transformation. The rheological behavior of these liquids is found to progressively deviate from that of a "normal" network liquid with increasing x in this composition range. While the liquids with compositions $30 \leq x \leq 40$ behave as simple liquids with a single bond scission/renewal relaxation process, the supercooled $P_{45}Se_{55}$ and $P_{50}Se_{50}$ liquids display an additional relaxation mode, which likely corresponds to a structural interconversion between ethylene-like $_{2/2}SeP\text{–}PSe_{2/2}$ units and P_4Se_3 molecules. In contrast to these normal network liquids that display a Maxwell frequency scaling of $G' \sim \omega^2$ and $G'' \sim \omega$ in the terminal region, the molecular liquids with $x \geq 63$ display an apparently anomalous scaling of $G' \sim \omega$ at frequencies below the G′-G" crossover. These viscoelastic spectra are simulated with the H-N function to obtain the distribution of the relaxation timescales in these liquids. This analysis indicates that the molecular liquids are characterized by rather broad relaxation time distribution compared to that characteristic of their network counterparts. These results are corroborated by the phase angle variation and the viscosity enhancement observed in the low frequency region below the dynamical onset all the way down to $\omega/\omega_{max} \sim 10^{-4}$. These results, when taken together, suggest the presence of ultraslow relaxation processes in these highly fragile molecular liquids and the lack of a purely viscous response similar to that displayed by gels at their critical point.

ACKNOWLEDGEMENTS

This study is supported by the National Science Foundation Grant NSF-DMR 1855176. Jason A. Brown is thanked for assistance with glass synthesis.

REFERENCES

[1] C.M. Roland, *Viscoleastic Behavior of Rubbery Materials* (Oxford University Press, Oxford, 2011).

[2] J.D. Ferry, *Viscoelastic Properties of Polymers* (John Wiley & Sons, 1980).

[3] M. Doi and S.F. Edwards, *The Theory of Polymer Dynamics* (Oxford University Press, Oxford, 1986).

[4] J.J. Mills, J. Non. Cryst. Solids **14**, 255 (1974).

[5] J. Tauke, T.A. Litovitz, and P.B. Macedo, J. Am. Ceram. Soc. **51**, 158 (1968).

[6] B. Mei, B. Zhuang, Y. Lu, L. An, and Z. Wang, J. Phys. Chem. Lett. **13**, 3957 (2022).

[7] S.P. Bierwirth, C. Gainaru, and R. Böhmer, J. Chem. Phys. **148**, 221102 (2018).

[8] R. Böhmer, C. Gainaru, and R. Richert, Phys. Rep. **545**, 125 (2014).

[9] C. Gainaru, R. Meier, S. Schildmann, C. Lederle, W. Hiller, E.A. Rössler, and R. Böhmer, Phys. Rev. Lett. **105**, 258303 (2010).

[10] W. Zhu, B.G. Aitken, and S. Sen, J. Chem. Phys. **148**, 111101 (2018).

[11] W. Zhu, B. Aitken, and S. Sen, J. Non. Cryst. Solids **534**, 119959 (2020).

[12] S. Sen, Y. Xia, W. Zhu, M. Lockhart, and B. Aitken, J. Chem. Phys. **150**, 144509 (2019).

[13] B. Yuan, B. Aitken, and S. Sen, J. Non. Cryst. Solids **559**, 120669 (2021).

[14] W. Zhu, I. Hung, Z. Gan, B. Aitken, and S. Sen, J. Non. Cryst. Solids **526**, 119698 (2019).

[15] S. Sen, W. Zhu, B. Yuan, and B.G. Aitken, J. Chem. Phys. **153**, 134504 (2020).

[16] S. Aime, L. Cipelletti, and L. Ramos, J. Rheol. **62**, 1429 (2018).

[17] P. Sollich, F. Lequeux, P. Hébraud, and M.E. Cates, Phys. Rev. Lett. **78**, 2020 (1997).

[18] B. Yuan, B. Aitken, I. Hung, Z. Gan, and S. Sen, J. Phys. Chem. B **125**, 13057 (2021).

[19] A. Bytchkov, F. Fayon, D. Massiot, L. Hennet, and D.L. Price, Phys. Chem. Chem. Phys. **12**, 1535 (2010).

[20] D.G. Georgiev, M. Mitkova, P. Boolchand, G. Brunklaus, H. Eckert, and M. Micoulaut, Phys. Rev. B **64**, 134204 (2001).

[21] R.T. Phillips and M.K. Ellis, J. Non. Cryst. Solids **164–166**, 135 (1993).

[22] D. Lathrop and H. Eckert, Phys. Rev. B **43**, 7279 (1991).

[23] D. Lathrop and H. Eckert, J. Am. Chem. Soc. **112**, 9017 (1990).

[24] D. Lathrop and H. Eckert, J. Phys. Chem. **93**, 7895 (1989).

[25] D. Lathrop and H. Eckert, J. Non. Cryst. Solids **106**, 417 (1988).

[26] R. Maxwell and H. Eckert, J. Phys. Chem. **99**, 4768 (1995).

[27] R. Maxwell and H. Eckert, J. Am. Chem. Soc. **116**, 682 (1994).

[28] R. Maxwell and H. Eckert, J. Am. Chem. Soc. **115**, 4747 (1993).

[29] J.E. Martin and D. Adolf, Annu. Rev. Phys. Chem. **42**, 311 (1991).

[30] K. Ninomiya and J. Ferry, J. Colloid Sci. **14**, 36 (1959).

[31] D.C. Kaseman, O. Gulbiten, B.G. Aitken, and S. Sen, J. Chem. Phys. **144**, 174501 (2016).

[32] P. Mondal, P. Lunkenheimer, R. Böhmer, A. Loidl, F. Gugenberger, P. Adelmann, and C.

Meingast, J. Non. Cryst. Solids **172–174**, 468 (1994).

[33] T. Chattopadhyay, C. Carlone, A. Jayaraman, and H.G. V. Schnering, J. Phys. Chem. Solids **43**, 277 (1982).

[34] S. Havriliak and S. Negami, Polymer. **8**, 161 (1967).

[35] P.G. Debenedetti and F.H. Stillinger, Nature **410**, 259 (2001).

[36] J.C. Mauro, Y. Yue, A.J. Ellison, P.K. Gupta, and D.C. Allan, Proc. Natl. Acad. Sci. **106**, 19780 (2009).

[37] C. Zhang, L. Hu, Y. Yue, and J.C. Mauro, J. Chem. Phys. **133**, 14508 (2010).

[38] E.I. Kim and G.M. Orlova, J. Appl. Chem. USSR **47**, 1081 (1974).

Figure Captions

Figure 1. (a) Frequency dependence of G′ (solid line) and G″ (dashed line) at different temperatures for P_xSe_{100-x} supercooled liquids. (b) Master curves of G′(ω) (black squares) and G″(ω) (red circles) of P_xSe_{100-x} supercooled liquids with the reference temperatures for TTS listed alongside the compositions in each panel. Solid straight-line segments mark the slopes n in different frequency regions.

Figure 2. Relaxation spectra H(τ) of supercooled $P_{30}Se_{70}$ network liquid (filled squares) and molecular $P_{63}Se_{37}$ liquid (empty squares) at 110°C and 30°C, respectively. H(τ) of supercooled molecular $Ge_3As_{52}S_{45}$ liquid (open diamonds) from a previous study is shown for comparison.[15]

Figure 3. Viscoelastic spectra G′(ω) (empty squares) and G″(ω) (empty circles) of $P_{30}Se_{70}$ network (left panel) and $P_{63}Se_{37}$ molecular (right panel) liquids fitted with the H-N function (Eq. 2, dashed line). The fitting parameters α and β are listed in each plot.

Figure 4. The probability density function of H-N log-relaxation time $h_{HN}(\log\tau)$ for $P_{30}Se_{70}$ network (dashed line) and $P_{63}Se_{37}$ molecular liquids (solid line) calculated using Eq. 3 (see text for details).

Figure 5. Temperature dependence of viscosity η of binary P_xSe_{100-x} liquids. Filled symbols are experimental data obtained in present study and the open symbols are data taken from a previous study.[38] Inset shows compositional variation of T_g of these glasses from previous reports in the literature.[18,38]

Figure 6. Scaled dynamic viscosity $Z(\omega)$ as a function of normalized frequency ω/ω_{max} of P_xSe_{100-x} liquids. Corresponding temperatures are shown in parentheses alongside each composition.

Figure 7. vGP plot of phase angle δ vs. $|G^*|$ of $P_{30}Se_{70}$ network liquid (black squares) and molecular $P_{63}Se_{37}$ liquid (red squares). Data for molecular $Ge_3As_{52}S_{45}$ liquid (blue triangles) from a previous study is shown for comparison.[15]

Fig. 1a

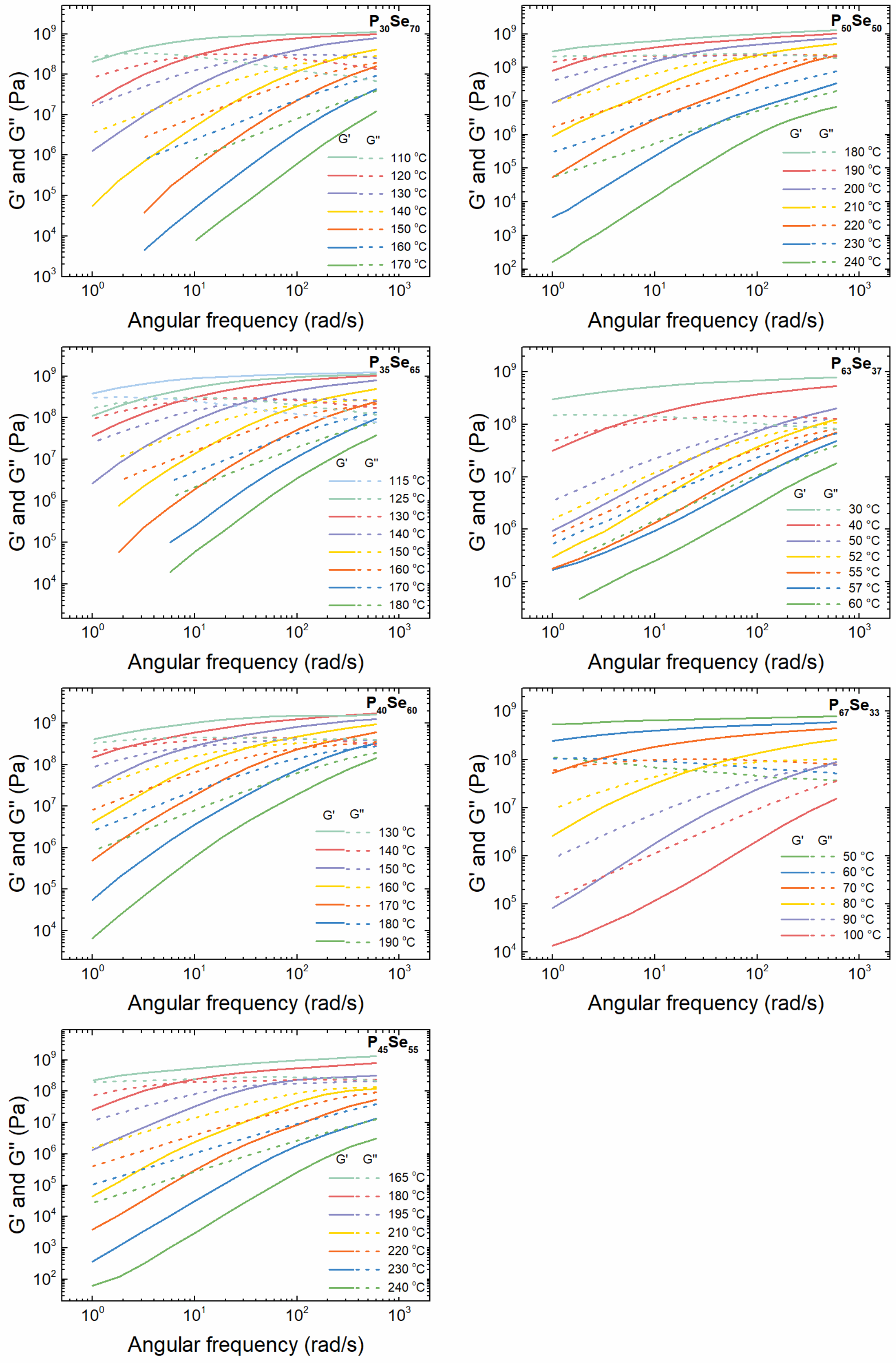

$P_{30}Se_{70}$
G' G"
110 °C
120 °C
130 °C
140 °C
150 °C
160 °C
170 °C
$P_{50}Se_{50}$
G' G"
180 °C
190 °C
200 °C
210 °C
220 °C
230 °C
240 °C
$P_{35}Se_{65}$
G' G"
115 °C
125 °C
130 °C
140 °C
150 °C
160 °C
170 °C
180 °C
$P_{63}Se_{37}$
G' G"
30 °C
40 °C
50 °C
52 °C
55 °C
57 °C
60 °C
$P_{40}Se_{60}$
G' G"
130 °C
140 °C
150 °C
160 °C
170 °C
180 °C
190 °C
$P_{67}Se_{33}$
G' G"
50 °C
60 °C
70 °C
80 °C
90 °C
100 °C
$P_{45}Se_{55}$
G' G"
165 °C
180 °C
195 °C
210 °C
220 °C
230 °C
240 °C
G' and G" (Pa)
Angular frequency (rad/s)
10^0 10^1 10^2 10^3
10^2 10^3 10^4 10^5 10^6 10^7 10^8 10^9

Fig. 1b

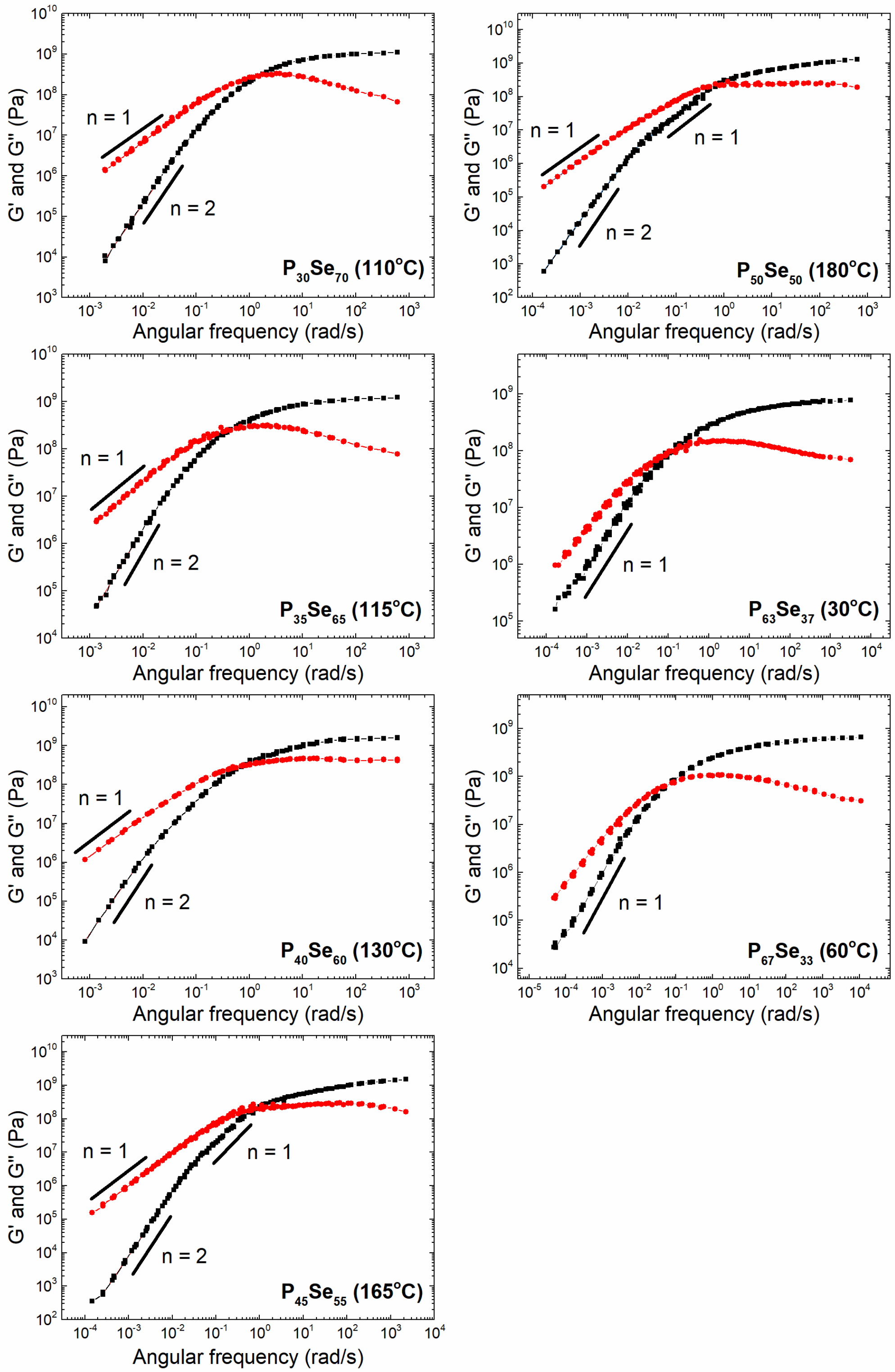

G' and G'' (Pa)
Angular frequency (rad/s)
n = 1
n = 2
$P_{30}Se_{70}$ (110°C)
$P_{50}Se_{50}$ (180°C)
$P_{35}Se_{65}$ (115°C)
$P_{63}Se_{37}$ (30°C)
$P_{40}Se_{60}$ (130°C)
$P_{67}Se_{33}$ (60°C)
$P_{45}Se_{55}$ (165°C)
10^{-5}
10^{-4}
10^{-3}
10^{-2}
10^{-1}
10^{0}
10^{1}
10^{2}
10^{3}
10^{4}
10^{5}
10^{6}
10^{7}
10^{8}
10^{9}
10^{10}

Fig. 2

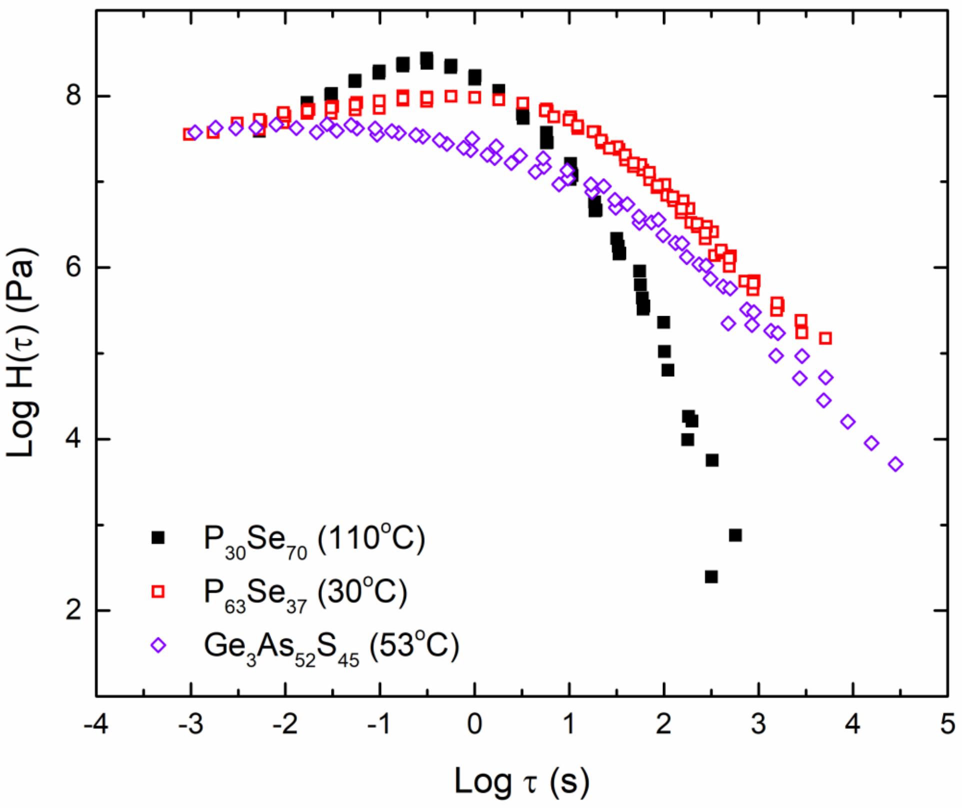
Log H(τ) (Pa)
Log τ (s)
8
6
4
2
-4
-3
-2
-1
0
1
2
3
4
5
$P_{30}Se_{70}$ (110°C)
$P_{63}Se_{37}$ (30°C)
$Ge_3As_{52}S_{45}$ (53°C)

Fig. 3

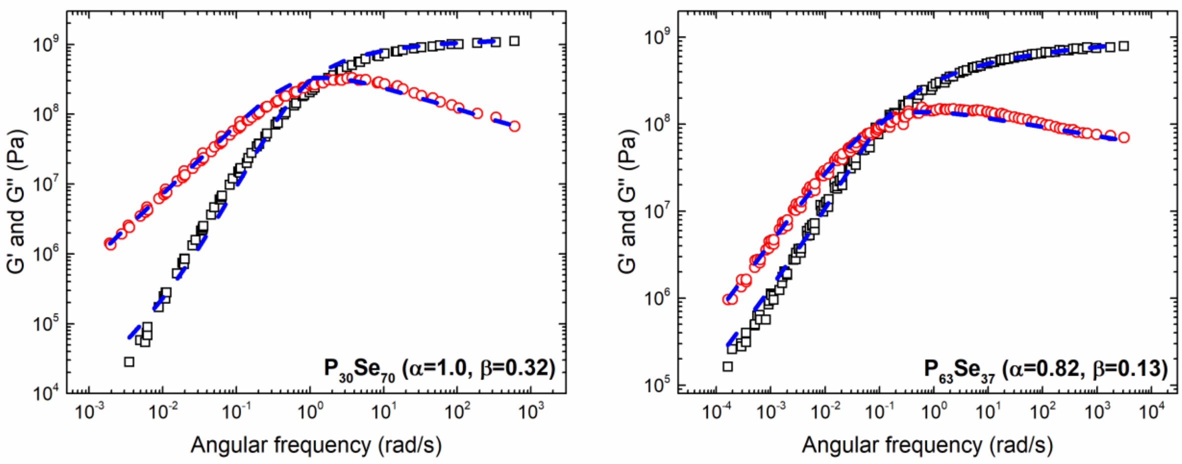
G' and G'' (Pa)
Angular frequency (rad/s)
$P_{30}Se_{70}$ (α=1.0, β=0.32)
10^4
10^5
10^6
10^7
10^8
10^9
10^{-3}
10^{-2}
10^{-1}
10^0
10^1
10^2
10^3
G' and G'' (Pa)
Angular frequency (rad/s)
$P_{63}Se_{37}$ (α=0.82, β=0.13)
10^5
10^6
10^7
10^8
10^9
10^{-4}
10^{-3}
10^{-2}
10^{-1}
10^0
10^1
10^2
10^3
10^4

Fig. 4

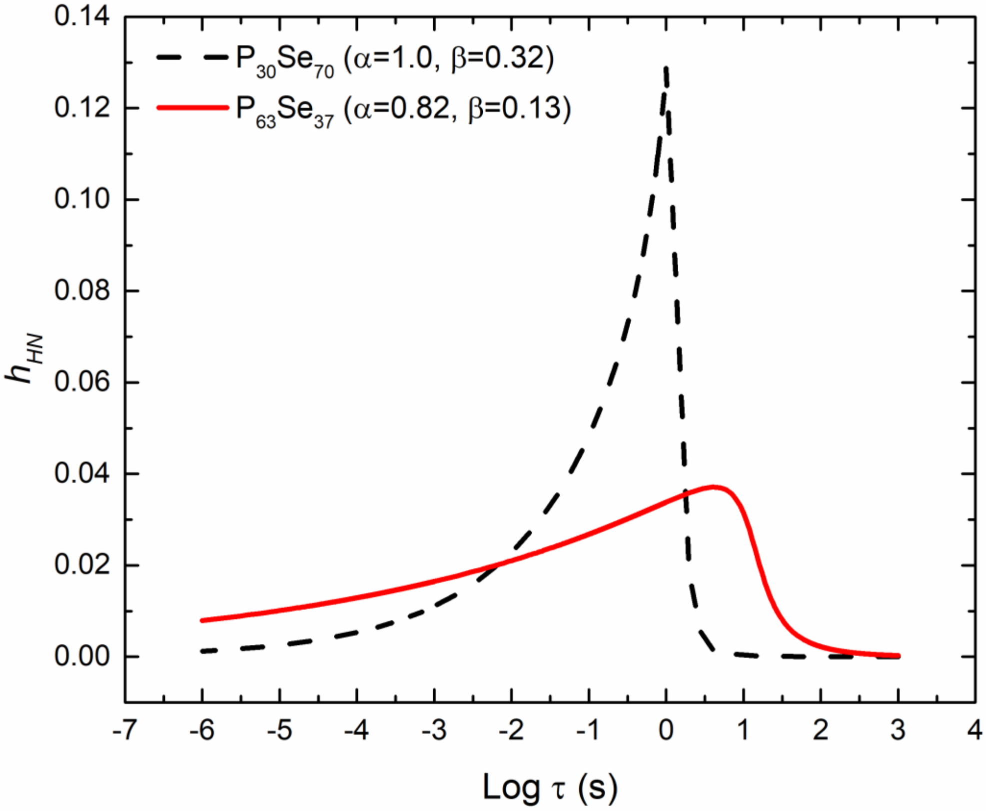

0.14
0.12
0.10
0.08
0.06
0.04
0.02
0.00
h_{HN}
-7
-6
-5
-4
-3
-2
-1
0
1
2
3
4
Log τ (s)
$P_{30}Se_{70}$ (α=1.0, β=0.32)
$P_{63}Se_{37}$ (α=0.82, β=0.13)

Fig. 5.

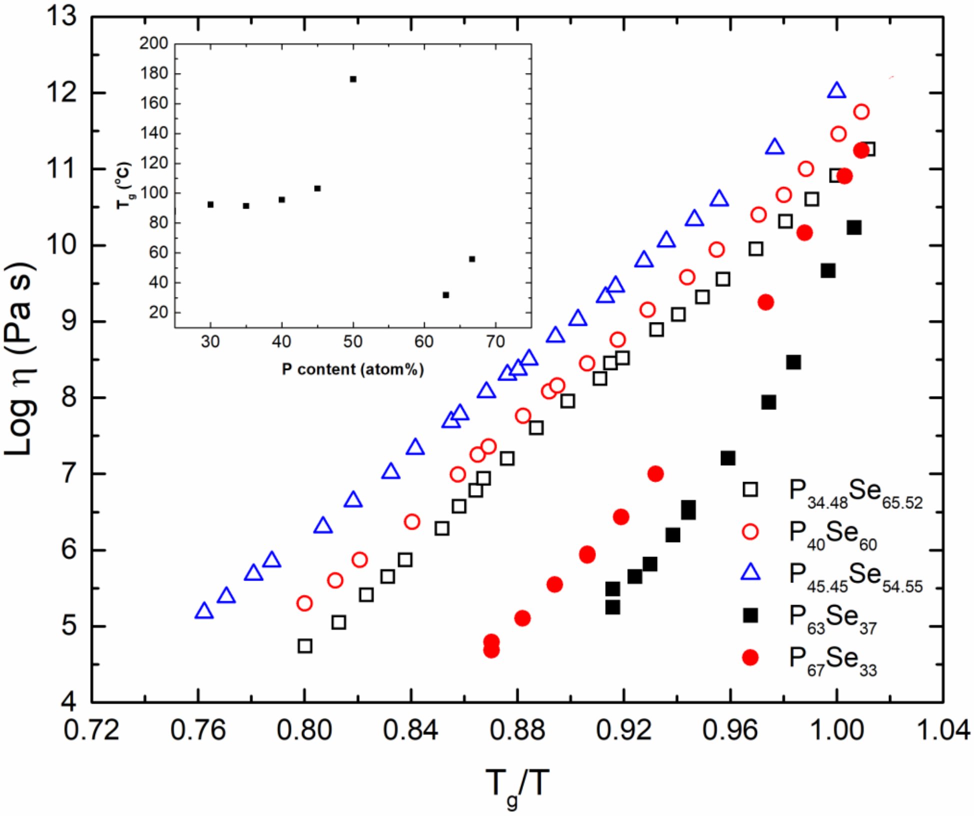

Log η (Pa s)
13
12
11
10
9
8
7
6
5
4
0.72
0.76
0.80
0.84
0.88
0.92
0.96
1.00
1.04
T_g/T
T_g (°C)
200
180
160
140
120
100
80
60
40
20
30
40
50
60
70
P content (atom%)
$P_{34.48}Se_{65.52}$
$P_{40}Se_{60}$
$P_{45.45}Se_{54.55}$
$P_{63}Se_{37}$
$P_{67}Se_{33}$

Fig. 6

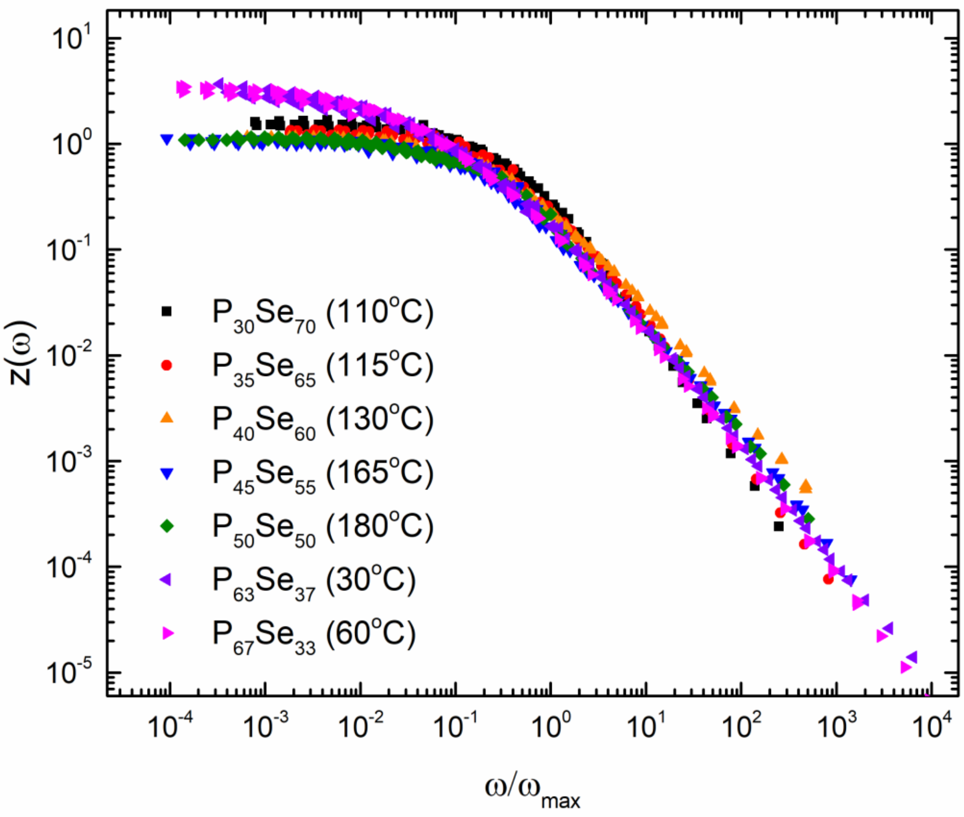

10^1
10^0
10^{-1}
10^{-2}
10^{-3}
10^{-4}
10^{-5}
$z(\omega)$
10^{-4}
10^{-3}
10^{-2}
10^{-1}
10^0
10^1
10^2
10^3
10^4
ω/ω_{max}
■ $P_{30}Se_{70}$ (110°C)
● $P_{35}Se_{65}$ (115°C)
▲ $P_{40}Se_{60}$ (130°C)
▼ $P_{45}Se_{55}$ (165°C)
◆ $P_{50}Se_{50}$ (180°C)
◀ $P_{63}Se_{37}$ (30°C)
▶ $P_{67}Se_{33}$ (60°C)

Fig. 7

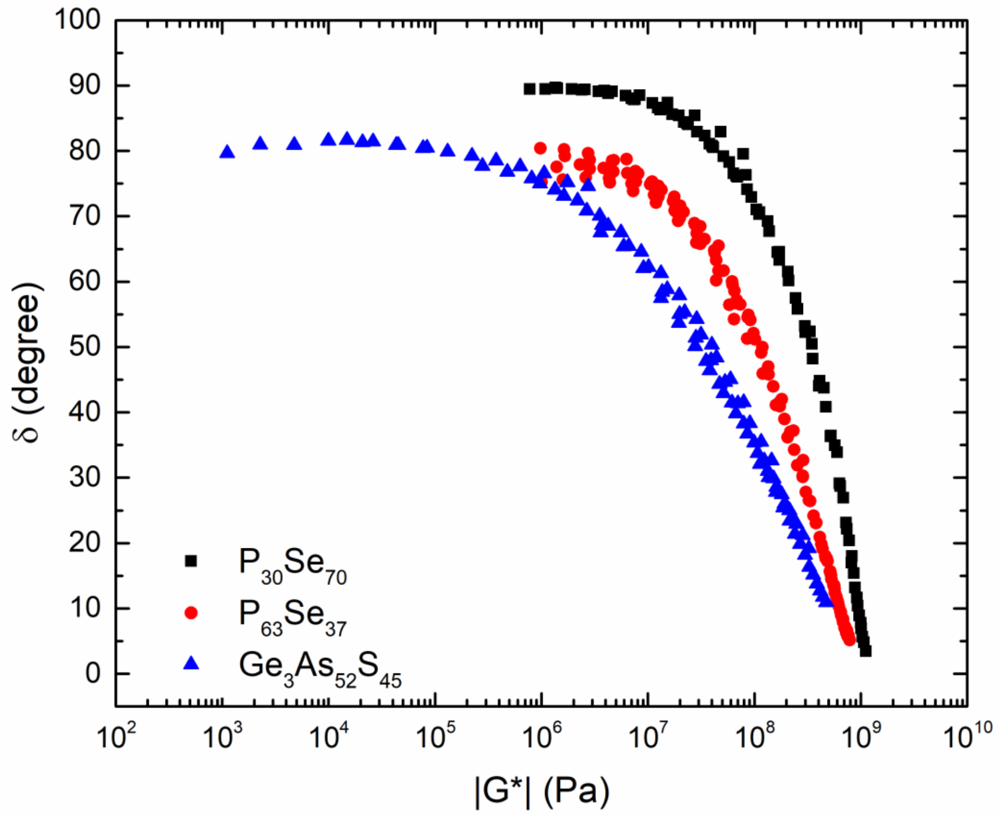
δ (degree)
100
90
80
70
60
50
40
30
20
10
0
10^2
10^3
10^4
10^5
10^6
10^7
10^8
10^9
10^{10}
|G*| (Pa)
$P_{30}Se_{70}$
$P_{63}Se_{37}$
$Ge_3As_{52}S_{45}$